J. Austral. Math. Soc. **20** (Series B) (1978), 385–400

THE ELASTODYNAMIC GREEN'S TENSOR FOR THE 2D HALF-SPACE

PETER W. BUCHEN

(Received 6 March 1978)

Abstract

An exact algebraic representation for the 2D elastodynamic Green's tensor is derived. A new displacement potential decomposition is employed which yields, in conjunction with the Pekeris–Cagniard–de Hoop method, the exact representation. The first motions of the major arrivals are evaluated in terms of their polarizations, radiation patterns, geometrical spreading and wave-front singularities. The tensorial components of the Rayleigh wave on the free surface are found and solutions for dipolar line source discussed. We also investigate diffracted phases first noticed by Lapwood in his 1949 paper [13].

Introduction

Ever since the publication of Horace Lamb's epic 1904 paper [12], elastodynamic half-space problems under varying source conditions have been referred to as *Lamb's problem*. Lamb, himself, considered only the surface displacement generated by vertical and horizontal periodic line sources situated on the free surface of the elastic half-space. He was able to demonstrate the arrival of the familiar sequence of P, S and Rayleigh waves. The solution for a pulse-type source was then synthesized from the periodic one.

Nankano [14] first considered the problem of a buried source and Lapwood [13] obtained detailed asymptotic representations for all the principal phases associated with this case. Lapwood's solution predicted various diffracted phases largely ignored in later treatments. We shall discuss the reality of these non-least time phases in this paper (Section 11).

A new technique developed independently by Cagniard [4] in 1939 and Pekeris in 1940 allowed for direct evaluation of the solution for the pulse-type sources. The method, in addition, provided a closed form exact representation for the solution of the Lamb's problem. Pekeris, initially considered the surface pulse and only later [15, 16] extended it to include the buried pulse-type source. Two

elegant demonstrations of the Pekeris–Cagniard method should be noted. Garnir [7] applied the method successfully to a corresponding acoustic problem and Garvin [8] to the elastic buried line source problem.

The method was much improved and simplified by de Hoop [5] and most subsequent contributions have employed de Hoop's modification. A comprehensive treatment of the 3D Green's tensor has recently been published by Johnson [10]. However, the 3D case does not lend itself to the methods employed here, which exploits to the hilt the assumed two-dimensionality. Furthermore, the 2D case allows for a neat closed form exact representation.

In Part A of this paper we derive an expression for this exact algebraic representation. We employ a new potential decomposition for the displacements and arrive at the solution via the Pekeris–Cagniard–de Hoop method. We believe this study to be worth while for the following reasons. Firstly, there is no obvious way to relate previously published solutions of the Lamb's problem to that of the Green's tensor, which requires a very specific source function. Secondly, once the precise Green's tensor has been found, the solution for any other source can be found by convolution. Thirdly, a knowledge of the Green's tensor is needed in certain Born-type scattering problems, which are beginning to find importance in seismology (for example, King *et al.* [11]).

In Part B we investigate the principal arrivals and derive their first motions. In this, we follow the approach of Gilbert and Knopoff [9]. Expressions in terms of polarization vectors, source directivity (radiation pattern), geometrical spreading and wave-front singularities are derived. The tensorial components of the Rayleigh wave on the free-surface are evaluated and we discuss Lapwood's diffracted phases and finally comment on the nature of the solutions for dipolar sources. This last section has been investigated in more detail by Burridge *et al.* [3] and Ben-Menahem *et al.* [1].

PART A

1. The equations of motion

In a uniform, isotropic elastic solid of density ρ and elastic constants κ, μ the elastic displacement vector $\mathbf{u}(x,t)$ satisfies

$$\rho\frac{\partial^2\mathbf{u}}{\partial t^2} = (\kappa+\tfrac{4}{3}\mu)\,\nabla(\nabla\cdot\mathbf{u}) - \mu\nabla\times(\nabla\times\mathbf{u}) + \rho\mathbf{F}, \tag{1.1}$$

where $\mathbf{F}(\mathbf{x},t)$ defines the distribution of internal body forces.

By definition, the Green's tensor $G_{ik}(\mathbf{x}|\mathbf{y};t)$ is the elastic displacement corresponding to the body force

$$\mathbf{F} = F_{ik} = Q\delta_{ik}\,\delta(t)\,\delta(\mathbf{x}-\mathbf{y}), \tag{1.2}$$

https://doi.org/10.1017/S1446181100001772 Published online by Cambridge University Press

where $(\mathbf{y}, k)$ refer to the source and $(\mathbf{x}, i)$ to the field point respectively.

Much simplification can be made by exploiting the assumed two-dimensionality of the problem. Let us define the 2D gradient and rotation operators

$$\partial^i = \frac{\partial}{\partial x_i} = \left(\frac{\partial}{\partial x_1}, \frac{\partial}{\partial x_2}\right); \quad d^i = \varepsilon_{ij3}\frac{\partial}{\partial x_j} = \left(\frac{\partial}{\partial x_2}, -\frac{\partial}{\partial x_1}\right). \tag{1.3}$$

Then the Green's tensor formally satisfies the equation

$$\left[\delta_{ij}\frac{\partial^2}{\partial t^2} - \alpha^2\,\partial^i\,\partial^j - \beta^2\,d^i\,d^j\right] G_{jk} = F_{ik}, \tag{1.4}$$

where α, β are the usual P and S wave speeds. We choose coordinates so that (1.4) holds in the half-space $x_2 > 0$. The source is assumed internal so that $y_2 > 0$ also. For boundary conditions we shall take the usual conditions of zero surface traction on $x_2 = 0$ (that is, a free surface) and vanishing of all quantities as $x_2 \to \infty$. Since the stress components can be written in the form

$$\tau_{ij} = (\kappa - \tfrac{2}{3}\mu)(\partial^k u_k)\delta_{ij} + \mu(\partial^i u_j + \partial^j u_i),$$

the surface boundary condition $\tau_{i2} = 0$ on $x_2 = 0$ becomes

$$\mathscr{B}_{ij}\,G_{jk} = \left[\left(\frac{\alpha^2}{\beta^2} - 2\right)\delta_{i2}\,\partial^j + \delta_{ij}\,\partial^{(2)} + \delta_{2j}\,\partial^i\right] G_{jk} = 0. \tag{1.5}$$

2. The potential decomposition

Motivated by the realization that G_{ik} can be treated as a vector for fixed source direction k, we write

$$G_{ik} = \partial^i\,\Phi_k + d^i\,\Psi_k. \tag{2.1}$$

Similarly, we may regard Φ_k, Ψ_k as components of a vector field over source coordinates $\mathbf{y}$, so that

$$\Phi_k = \partial_0^k\,\phi + d_0^k\,\Omega; \quad \Psi_k = \partial_0^k\,\chi + d_0^k\,\psi, \tag{2.2}$$

where the subscripts denote the operations (1.3) taken with respect to source coordinates.

We thus have a representation for G_{ik} in terms of four scalar potentials

$$G_{ik} = \partial^i\,\partial_0^k\,\phi + \partial^i\,d_0^k\,\Omega + d^i\,\partial_0^k\,\chi + d^i\,d_0^k\,\psi. \tag{2.3}$$

This representation for the Green's tensor is new and makes for much simplification since it is always easier to deal with scalar equations. The four potentials in fact correspond to the four possible combinations of P and S waves leaving the source and arriving at the field point.

The reciprocity of the Green's tensor (Burridge and Knopoff [2])

$$G_{ik}(\mathbf{x}|\mathbf{y}; t) = G_{ki}(\mathbf{y}|\mathbf{x}; t)$$

https://doi.org/10.1017/S1446181100001772 Published online by Cambridge University Press

imposes the following source-receiver symmetries on the potentials:

$$\left.\begin{aligned}\phi(\mathbf{x}|\mathbf{y};t) &= \phi(\mathbf{y}|\mathbf{x};t);\\ \Omega(\mathbf{x}|\mathbf{y};t) &= \chi(\mathbf{y}|\mathbf{x};t);\\ \psi(\mathbf{x}|\mathbf{y};t) &= \psi(\mathbf{y}|\mathbf{x};t).\end{aligned}\right\} \tag{2.4}$$

Thus only three of the potentials are in fact independent. We might have expected that the *SP* and *PS* phases are reciprocal.

We can decompose the source function F_{ik} in exactly the same way as

$$F_{ik} = (Q/2\pi)\,\delta(t)\,[\partial^i\,\partial_0^k + d^i\,d_0^k]\ln r, \tag{2.5}$$

where we have used the well-known 2D result:

$$\delta(\mathbf{x}-\mathbf{y}) = -(1/2\pi)\,\nabla^2 \ln r; \quad r = |\mathbf{x}-\mathbf{y}|.$$

Substitution of (2.3) and (2.5) into the equation of motion (1.4) now leads to the equivalent set of scalar equations for $x_2>0$, $t>0$:

$$\left.\begin{aligned}\nabla^2\phi - \frac{1}{\alpha^2}\frac{\partial^2\phi}{\partial t^2} &= -\frac{Q}{2\pi\alpha^2}\delta(t)\ln r,\\ \nabla^2\Omega - \frac{1}{\alpha^2}\frac{\partial^2\Omega}{\partial t^2} &= 0,\\ \nabla^2\chi - \frac{1}{\beta^2}\frac{\partial^2\chi}{\partial t^2} &= 0,\\ \nabla^2\psi - \frac{1}{\beta^2}\frac{\partial^2\psi}{\partial t^2} &= -\frac{Q}{2\pi\beta^2}\delta(t)\ln r.\end{aligned}\right\} \tag{2.6}$$

The potentials are coupled in pairs through the boundary conditions

$$\mathscr{B}_i(\phi,\chi) = \mathscr{B}_i(\Omega,\psi) = 0 \quad \text{on } x_2 = 0, \tag{2.7}$$

where we have defined $\mathscr{B}_i(\phi,\chi) = \mathscr{B}_{ij}(\partial^j\phi + d\ \chi)$.

3. Transformation of the equations and their particular solutions

Let us introduce a Laplace transform in the time domain defined by

$$\bar{\phi}(\mathbf{x}|\mathbf{y};\sigma) = \int_0^\infty \phi(\mathbf{x}|\mathbf{y};t)\exp(-\sigma t)\,dt, \tag{3.1}$$

with σ real and positive.

The system (2.6) then transforms to equations of the form:

$$\nabla^2\bar{\phi} - \frac{\sigma^2}{\alpha^2}\bar{\phi} = -\frac{Q}{2\pi\alpha^2}\ln r, \quad \text{etc.} \tag{3.2}$$

https://doi.org/10.1017/S1446181100001772 Published online by Cambridge University Press

This has the particular solution (with correct behaviour at $r = 0$)

$$\bar{\phi}_0(\mathbf{x}|\mathbf{y};\sigma) = \frac{Q}{2\pi\sigma^2}\left[\ln r - K_0\left(\frac{\sigma r}{\alpha}\right)\right], \tag{3.3}$$

where K_0 is the modified Bessel function of the second kind, of order zero. There will also be a particular solution $\bar{\psi}_0(x|y;t)$ with α simply replaced by β. The equations for $\bar{\Omega}$ and $\bar{\chi}$ are homogeneous, so they will not involve particular solutions.

However, it is clear that the terms in $\ln r$ give a contribution to $\bar{G}_{ik}$ equal to

$$\frac{Q}{2\pi\sigma^2}[\partial^l \partial_0^k + d^l d_0^k]\ln r = \frac{Q}{\sigma^2}\delta(\mathbf{x}-\mathbf{y}),$$

which vanishes for all points such that $r \neq 0$. Thus for $r \neq 0$, we may take particular solutions

$$\bar{\phi}_0 = -\frac{Q}{2\pi\sigma^2}K_0\left(\frac{\sigma r}{\alpha}\right); \quad \bar{\psi}_0 = -\frac{Q}{2\pi\sigma^2}K_0\left(\frac{\sigma r}{\beta}\right). \tag{3.4}$$

These correspond, of course, to the direct or radiated P and S waves respectively.

4. Plane wave representation of the solution

A suitable integral representation of (3.4) for our purpose is

$$\bar{\phi}_0 = -\frac{Q}{2\pi\sigma^2}\operatorname{Im}\left\{\int_0^{i\infty}\exp\left[-\xi(x_1-y_1)-\nu_\alpha|x_2-y_2|\right]\frac{d\xi}{\nu_\alpha}\right\}, \tag{4.1}$$

where $\nu_\alpha = (\sigma^2/\alpha^2 - \xi^2)^{\frac{1}{2}}$; $\operatorname{Re}\nu_\alpha \geqslant 0$ and the path of integration may lie within the strip $|\operatorname{Re}\xi| < \sigma/\alpha$ of the complex ξ-plane.

We construct homogeneous solutions for the transformed potentials in the following manner:

$$\left.\begin{aligned}
\bar{\phi}_1 &= \frac{Q}{2\pi\sigma^2}\operatorname{Im}\int_0^{i\infty} A(\xi)\exp\left[-\xi(x_1-y_1)-\nu_\alpha(x_2+y_2)\right]\frac{d\xi}{\nu_\alpha};\\
\bar{\Omega} &= \frac{Q}{2\pi\sigma^2}\operatorname{Im}\int_0^{i\infty} B(\xi)\exp\left[-\xi(x_1-y_1)-\nu_\alpha x_2-\nu_\beta y_2\right]d\xi;\\
\bar{\chi} &= \frac{-Q}{2\pi\sigma^2}\operatorname{Im}\int_0^{i\infty} C(\xi)\exp\left[-\xi(x_1-y_1)-\nu_\beta x_2-\nu_\alpha y_2\right]d\xi;\\
\bar{\psi}_1 &= \frac{Q}{2\pi\sigma^2}\operatorname{Im}\int_0^{i\infty} D(\xi)\exp\left[-\xi(x_1-y_1)-\nu_\beta(x_2+y_2)\right]\frac{d\xi}{\nu_\beta}.
\end{aligned}\right\} \tag{4.2}$$

https://doi.org/10.1017/S1446181100001772 Published online by Cambridge University Press

The constants A, B, C, D are determined through the transformed boundary conditions on $x_2 = 0$

$$\mathscr{B}_i(\bar{\phi}_1, \bar{\chi}) = -\mathscr{B}_i(\bar{\phi}_0, 0); \quad \mathscr{B}_i(\bar{\Omega}, \bar{\psi}_1) = -\mathscr{B}_i(0, \bar{\psi}_0). \tag{4.3}$$

These are four linear algebraic equations with solution

$$A = D = S/R; \quad B = C = T/R, \tag{4.4}$$

where

$$\left.\begin{aligned} R &= R(\xi, \sigma) = (\nu_\beta^2 - \xi^2)^2 + 4\xi^2 \nu_\alpha \nu_\beta; \\ S &= S(\xi, \sigma) = (\nu_\beta^2 - \xi^2)^2 - 4\xi^2 \nu_\alpha \nu_\beta; \\ T &= T(\xi, \sigma) = 4\xi(\nu_\beta^2 - \xi^2). \end{aligned}\right\} \tag{4.5}$$

5. The Pekeris–Cagniard–de Hoop representation

We seek to further modify the plane wave representation (4.1) and (4.2) with the ultimate goal of obtaining exact expressions for the potentials and hence the Green's tensor.

Firstly, with the similarity transformation

$$\xi = p\sigma, \tag{5.1}$$

we get some simplification because of the homogeneity of the integrands. The parameter p may be called the complex surface slowness. In an obvious notation we find

$$\left.\begin{aligned} \nu_\alpha &= \sigma\eta_\alpha(p); \quad \nu_\beta = \sigma\eta_\beta(p); \\ R(\xi, \sigma) &= \sigma^4 R(p); \quad S(\xi, \sigma) = \sigma^4 S(p); \quad T(\xi, \sigma) = \sigma^3 T(p). \end{aligned}\right\} \tag{5.2}$$

Let us define complex slowness vectors with components

$$\boldsymbol{\pi}^\pm = (p;\ \pm\eta_\alpha); \quad \mathbf{s}^\pm = (p;\ \pm\eta_\beta); \quad \boldsymbol{\sigma}^\pm = (\pm\eta_\beta;\ -p), \tag{5.3}$$

where $|\boldsymbol{\pi}^\pm| = 1/\alpha$ and $|\mathbf{s}^\pm| = |\boldsymbol{\sigma}^\pm| = 1/\beta$. Note that $\boldsymbol{\sigma}^\pm$ is the orthogonal complement of $\mathbf{s}^\pm$.

Now we define complex travel times for each phase as follows:

$$\left.\begin{aligned} \tau^P &= \boldsymbol{\pi}^\pm \cdot (\mathbf{x} - \mathbf{y}); \qquad \tau^S = \mathbf{s}^\pm \cdot (\mathbf{x} - \mathbf{y}); \qquad x_2 \gtrless y_2; \\ \tau^{PP} &= \boldsymbol{\pi}^+ \cdot \mathbf{x} - \boldsymbol{\pi}^- \cdot \mathbf{y}; \quad \tau^{SP} = \boldsymbol{\pi}^+ \cdot \mathbf{x} - \mathbf{s}^- \cdot \mathbf{y}; \\ \tau^{PS} &= \mathbf{s}^+ \cdot \mathbf{x} - \boldsymbol{\pi}^- \cdot \mathbf{y}; \quad \tau^{SS} = \mathbf{s}^+ \cdot \mathbf{x} - \mathbf{s}^- \cdot \mathbf{y}. \end{aligned}\right\} \tag{5.4}$$

https://doi.org/10.1017/S1446181100001772 Published online by Cambridge University Press

The chosen notation is of some significance. For instance, in the expression $\mathbf{s}^+ \cdot \mathbf{x} - \boldsymbol{\pi}^- \cdot \mathbf{y}$ for τ^{PS} we indicate that the phase leaves the source $\mathbf{y}$ in the negative direction (towards the free surface) as a P wave and arrives at the field point $\mathbf{x}$ in the positive direction (away from the free surface) as an S wave. The direct P and S waves may leave the source in either direction depending on whether $x_2 \gtrless y_2$.

Typically, we obtain representations of the type

$$\bar{\Omega}(SP) = \frac{Q}{2\pi\sigma^2} \operatorname{Im}\left\{\int_0^{i\infty} \frac{T(p)}{R(p)} \exp\left[-\sigma\tau^{SP}(\mathbf{x}|\mathbf{y};\, p)\right] dp\right\}, \quad |p| < \frac{1}{\alpha}. \tag{5.5}$$

The corresponding time-transformed component of the Green's tensor is then given by

$$\bar{G}_{ik}(SP) = \partial^i d_0^k \bar{\Omega} = -\frac{Q}{2\pi} \operatorname{Im} \int_0^{i\infty} \pi_i^+ \sigma_k^- \exp(-\sigma\tau^{SP}) \frac{T\, dp}{R}. \tag{5.6}$$

In a like manner we may obtain the other components

$$\bar{G}_{ik}(P) = \partial^i \partial_0^k \bar{\phi}_0; \quad \bar{G}_{ik}(S) = d_i d_0^k \bar{\psi}_0;$$

$$\bar{G}_{ik}(PP) = \partial^i \partial_0^k \bar{\phi}_1; \quad \bar{G}_{ik}(SS) = d^i d_0^k \bar{\psi}_1; \quad \bar{G}_{ik}(PS) = d^i \partial_0^k \bar{\chi}.$$

Secondly, we introduce into each of the integrands of type (5.6) a conformal transformation from the complex p-plane to the complex t-plane defined by

$$\tau(\mathbf{x}|\mathbf{y};\, p) = t, \tag{5.7}$$

where τ successively represents τ^P, τ^S, τ^{PP}, etc. The path in the complex p-plane which conformally corresponds to the positive real t-axis of the complex t-plane is called the *Pekeris–Cagniard–de Hoop path*, which we shall denote here by Γ.

If the original path in the p-plane from $|p| < 1/\alpha$ on real axis to $i\infty$ can be continuously distorted into Γ we will have a direct way of determining the time-dependent components of the Green's tensor. For example, in the case of the SP-phase of equation (5.6) we will have

$$\bar{G}_{ik}(SP) = \int_0^{\infty} \left\{-\frac{Q}{2\pi} \operatorname{Im}\left[\pi_i^+ \sigma_k^- \frac{T(p)}{R(p)} \dot{p}\right]_{\tau^{SP}=t}\right\} \exp(-\sigma t)\, dt. \tag{5.8}$$

Whence by the definition (3.1) of the Laplace transform we can write down, by inspection, the time-dependent Green's tensor $G_{ik}(SP)$. It is just the expression in $\{\}$.

For completeness, we give the final result. The Green's tensor $G_{ik}(\mathbf{x}|\mathbf{y};\, t)$ is the sum of the following components:

https://doi.org/10.1017/S1446181100001772 Published online by Cambridge University Press

$$\left.\begin{aligned}
G_{ik}(P) &= \frac{Q}{2\pi}\,\mathrm{Im}\,[\pi_i^{\pm}\,\pi_k^{\pm}\,\dot{p}/\eta_\alpha]_{\tau^P=t}, \quad x_2 \gtrless y_2;\\
G_{ik}(S) &= \frac{Q}{2\pi}\,\mathrm{Im}\,[\sigma_i^{\pm}\,\sigma_k^{\pm}\,\dot{p}/\eta_\beta]_{\tau^S=t}, \quad x_2 \gtrless y_2;\\
G_{ik}(PP) &= \frac{-Q}{2\pi}\,\mathrm{Im}\left[\pi_i^{+}\,\pi_k^{-}\,\frac{S(p)}{R(p)}\dot{p}/\eta_\alpha\right]_{\tau^{PP}=t};\\
G_{ik}(SS) &= \frac{-Q}{2\pi}\,\mathrm{Im}\left[\sigma_i^{+}\,\sigma_k^{-}\,\frac{S(p)}{R(p)}\dot{p}/\eta_\beta\right]_{\tau^{SS}=t};\\
G_{ik}(SP) &= \frac{-Q}{2\pi}\,\mathrm{Im}\left[\pi_i^{+}\,\sigma_k^{-}\,\frac{T(p)}{R(p)}\right]\dot{p}_{\tau^{SP}=t};\\
G_{ik}(PS) &= \frac{Q}{2\pi}\,\mathrm{Im}\left[\sigma_i^{+}\,\pi_k^{-}\,\frac{T(p)}{R(p)}\dot{p}\right]_{\tau^{PS}=t}.
\end{aligned}\right\} \tag{5.9}$$

Each square bracket in (5.9) is a function of the complex surface slowness $p = p(\mathbf{x}|\mathbf{y}; t)$ defined by the transformation (5.7). The term $\dot{p}$ can then be found by evaluating $\partial p/\partial t$. Since the function $R(p)$, $S(p)$ and $T(p)$ are algebraic, our solution is an exact algebraic representation for the 2D Green's tensor.

The following Sections are concerned with specific details of this basic solution.

PART B

6. The direct P and S waves

Let r, θ be plane polar coordinates of the field point $\mathbf{x}$ relative to the source $\mathbf{y}$ as origin. Then the equation $\tau^P = t$ can be solved for p as a complex function of r, θ and t. We find

$$p = \frac{t}{r}\cos\theta + \frac{it_\alpha}{r}|\sin\theta|, \tag{6.1}$$

where

$$t_\alpha = t_\alpha(r) = \begin{cases} (t^2 - r^2/\alpha^2)^{\frac{1}{2}}, & t > r/\alpha;\\ i(r^2/\alpha^2 - t^2)^{\frac{1}{2}}, & t < r/\alpha. \end{cases} \tag{6.2}$$

Then it follows that

$$\eta_\alpha = \frac{t}{r}|\sin\theta| - \frac{it_\alpha}{r}\cos\theta; \quad \dot{p} = i\eta_\alpha/t_\alpha; \quad \boldsymbol{\pi}^{\pm} = \frac{1}{r}[t\hat{\mathbf{r}} \pm it_\alpha\hat{\boldsymbol{\theta}}].$$

The complex p-plane has branch points at $p = \pm 1/\alpha$ with branch cuts, defined by $\mathrm{Re}\,\eta_\alpha = 0$, running along the real axis for $|p| > 1/\alpha$. Details are shown in Fig. 1.

https://doi.org/10.1017/S1446181100001772 Published online by Cambridge University Press

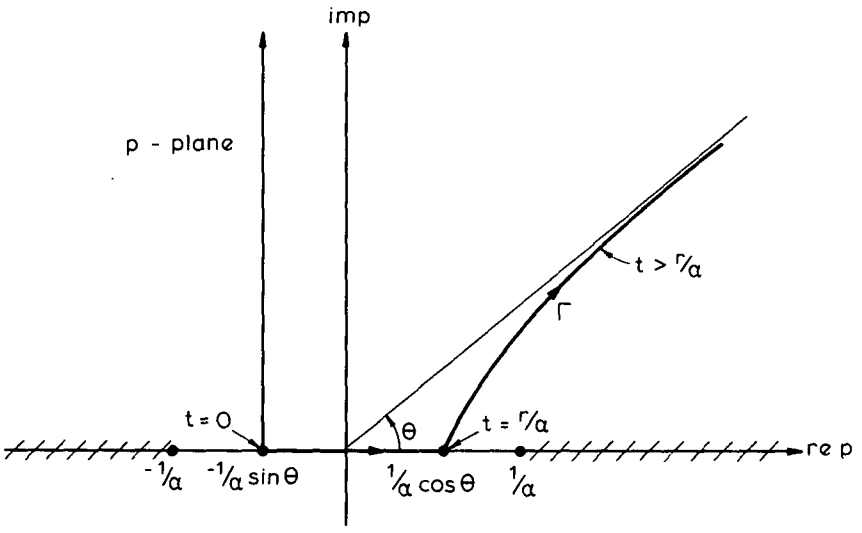

Fig. 1. The complex p-plane with branch cuts defined by $\mathrm{Re}\,\eta_\alpha = 0$ and the Pekeris–Cagniard–de Hoop path Γ defined by $\tau^p(\mathbf{x}|\mathbf{y};p) = t$; t real and positive.

Now all quantities in the expression for $G_{ik}(P)$ in equation (5.9) are real when $0 < t < r/\alpha$, so that in this range $G_{ik}(P) = 0$ as expected. We thus obtain the exact representation

$$G_{ik}(P) = \frac{Q}{2\pi r^2}\left[\frac{t^2}{t_\alpha}\hat{r}_i\hat{r}_k - t_\alpha\hat{\theta}_i\hat{\theta}_k\right]H(t-r/\alpha). \tag{6.3}$$

Similarly, for the direct S wave we find

$$G_{ik}(S) = \frac{Q}{2\pi r^2}\left[\frac{t^2}{t_\beta}\hat{\theta}_i\hat{\theta}_k - t_\beta\hat{r}_i\hat{r}_k\right]H(t-r/\beta) \tag{6.4}$$

with t_β defined as in (6.2). These expressions are a succinct form of the line-source radiated fields calculated by Eason *et al.* [6].

First motions are easily derived by expanding about $t \gtrsim r/\alpha$ and $t \gtrsim r/\beta$ respectively. We find, in this way,

$$\left.\begin{aligned} G_{ik}(P) &\sim \frac{Q}{(2\alpha)^{\frac{1}{2}}\pi}\hat{r}_i\hat{r}_k r^{-\frac{1}{2}}(t-r/\alpha)^{-\frac{1}{2}}; \\ G_{ik}(S) &\sim \frac{Q}{(2\beta)^{\frac{1}{2}}\pi}\hat{\theta}_i\hat{\theta}_k r^{-\frac{1}{2}}(t-r/\beta)^{-\frac{1}{2}}. \end{aligned}\right\} \tag{6.5}$$

We identify $\hat{r}_i$, $\hat{\theta}_i$ as unit P and S wave polarization vectors, indicating longitudinal and transverse particle motions respectively. The radiation patterns (source

https://doi.org/10.1017/S1446181100001772 Published online by Cambridge University Press

directivities) are (for fixed k) $\hat{r}_k$ and $\hat{\theta}_k$. The term $r^{-\frac{1}{2}}$ is due to geometrical spreading of the wave-fronts and the terms $(t-r/\alpha)^{-\frac{1}{2}}$, etc. are the usual 2D wave-front singularities.

Since the S to P amplitude ratio is $(\alpha/\beta)^{\frac{3}{2}}$, the simple line source generates S more efficiently than P.

Finally we observe that for t appreciably larger than r/β (and hence also r/α), there is a finite transverse component in the P wave and similarly a finite longitudinal component in the S wave. However, as $t\to\infty$, our solution indicates that their sum $G_{ik}(P)+G_{ik}(S)$ tends to zero.

7. The reflected PP and SS waves

Here we shall be principally concerned with the first motions of the reflected PP and SS phases. For this purpose, we now define polar coordinates r, θ relative to the image source $\mathbf{y}^* = (y_1, -y_2)$.

We leave out the details of the calculations, which in any case are very similar to that of Gilbert and Knopoff [9]. It is found that

$$G_{ik}(PP)\sim\frac{Q}{(2\alpha)^{\frac{3}{2}}\pi}\mathscr{R}_{PP}(\theta)\hat{r}_i\hat{r}_k^* r^{-\frac{1}{2}}(t-r/\alpha)^{-\frac{1}{2}} \tag{7.1}$$

for $t\gtrsim r/\alpha$ where

$$\mathscr{R}_{PP}(\theta)=\frac{4\sin\theta\cos^2\theta(\alpha^2/\beta^2-\cos^2\theta)^{\frac{1}{2}}-(\alpha^2/\beta^2-\cos^2\theta)^2}{4\sin\theta\cos^2\theta(\alpha^2/\beta^2-\cos^2\theta)^{\frac{1}{2}}+(\alpha^2/\beta^2-\cos^2\theta)^2} \tag{7.2}$$

is the usual PP-reflection coefficient for angle of incidence θ. These expressions are seen to be associated with the surface slowness $p\simeq(1/\alpha)\cos\theta$. For the SS wave, the first motion occurs at a surface slowness $p=(1/\beta)\cos\theta$ and immediately a difficulty arises.

Terms in the expression for $G_{ik}(SS)$ of equation (5.9) contain the factor $\eta_\alpha=(1/\alpha^2-p^2)^{\frac{1}{2}}$. This factor is real if $\theta>\theta_c$ where $\theta_c=\cos^{-1}(\beta/\alpha)$ is the critical angle. The first motions will be different in the two regions. We find, near $t\gtrsim r/\beta$,

$$G_{ik}(SS)\sim\frac{Q}{(2\beta)^{\frac{3}{2}}\pi}\mathscr{R}_{SS}^{\pm}(\theta)\hat{\theta}_i\hat{\theta}_k^* r^{-\frac{1}{2}}(t-r/\beta)^{-\frac{1}{2}} \tag{7.3}$$

where

$$\mathscr{R}_{SS}^{+}(\theta)=\frac{\cos^2 2\theta-4\sin\theta\cos^2\theta(\beta^2/\alpha^2-\cos^2\theta)^{\frac{1}{2}}}{\cos^2 2\theta+4\sin\theta\cos^2\theta(\beta^2/\alpha^2-\cos^2\theta)^{\frac{1}{2}}},\quad \theta>\theta_c \tag{7.4}$$

and

$$\mathscr{R}_{SS}^{-}(\theta)=\frac{\cos^4 2\theta-16\sin^2\theta\cos^4\theta(\cos^2\theta-\beta^2/\alpha^2)}{\cos^4 2\theta+16\sin^2\theta\cos^4\theta(\cos^2\theta-\beta^2/\alpha^2)},\quad \theta<\theta_c. \tag{7.5}$$

https://doi.org/10.1017/S1446181100001772 Published online by Cambridge University Press

Note that at critical incidence $\theta = \theta_c$, these reduce to $\mathscr{R}_{SS}^{+} = \mathscr{R}_{SS}^{-} = 1$ and the wave is totally internally reflected.

8. The *SPS*–head wave

All terms in the expression for $G_{ik}(SS)$ of equation (5.9) are real when $t < r/\beta$ and $\theta > \theta_c$ implying $G_{ik}(SS) = 0$ in this domain. However, for $t > r/\beta$, $\theta < \theta_c$ the factor η_α becomes pure imaginary in the interval of the real p-axis $1/\alpha < |p| < 1/\beta$. Thus it would appear that an additional disturbance sets in at $t = t_c$ corresponding to $p = 1/\alpha$. (See Fig. 2.) That is

$$t_c = \tau^{SS}\left(\mathbf{x}|\mathbf{y}; \frac{1}{\alpha}\right) = \frac{r}{\beta}\cos(\theta_c - \theta). \tag{8.1}$$

This is consistent with a ray-path which leaves the source $\mathbf{y}$ as an S wave at critical incidence, runs along the surface as a P wave and arrives at the field point $\mathbf{x}$ as an S wave, again at the critical angle. This is a diffracted wave called the *SPS*-head wave.

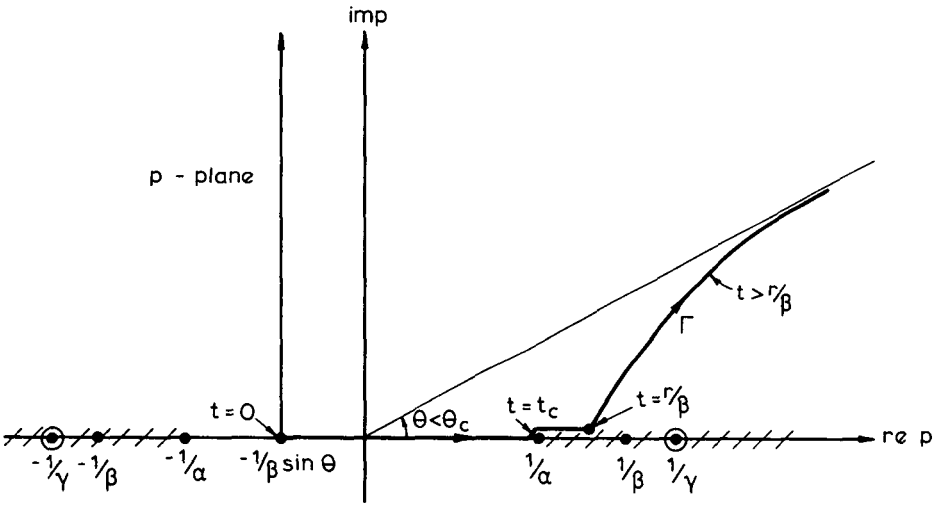

Fig. 2. The complex p-plane for $G_{ik}(SS)$ with branch cuts defined by $\mathrm{Re}\,\eta_\alpha = 0$ and $\mathrm{Re}\,\eta_\beta = 0$. The Pekeris–Cagniard–de Hoop path Γ defined by $\tau^{SS} = t$ indicates the arrival of the Head Wave at $p = 1/\alpha$ ($t = t_c$). The Rayleigh poles at $p = \pm 1/\gamma$ are also indicated.

Its first motion can be obtained in the usual manner by expanding about $t \gtrsim t_c$, corresponding to a surface slowness $p \sim 1/\alpha$. On simplification, we find

$$G_{ik}(SPS) \sim -\frac{(2\beta/\alpha)^{\frac{1}{2}}\, Q \sin\theta_c}{\pi \cos 2\theta_c}\, \hat{\theta}_i\, \hat{\theta}_k^{*}[r\sin(\theta_c - \theta)]^{-\frac{1}{2}}(t - t_c)^{\frac{1}{2}}, \tag{8.2}$$

https://doi.org/10.1017/S1446181100001772 Published online by Cambridge University Press

with the polarization vector $\hat{\theta}_i$ and source directivity $\hat{\theta}_k^*$ being evaluated at the critical angle. Note the $r^{-\frac{1}{2}}$ dependence and lack of singularity at the wave-front $t = t_c$.

9. The reflected *SP* and *PS* waves

In the Pekeris–Cagniard–de Hoop representation for the *SP* phase we shall set

$$p = \frac{t}{a}\cos\vartheta + \frac{it_\alpha(a)}{a}\sin\vartheta = \frac{t}{b}\cos\phi + \frac{it_\beta(b)}{b}\sin\phi, \tag{9.1}$$

which of course implies

$$\frac{\cos\vartheta}{a} = \frac{\cos\phi}{b}; \quad t_\alpha\frac{\sin\vartheta}{a} = t_\beta\frac{\sin\phi}{b}. \tag{9.2}$$

This immediately gives η_α and η_β as

$$\eta_\alpha = \frac{t}{a}\sin\vartheta - \frac{it_\alpha}{a}\cos\vartheta; \quad \eta_\beta = \frac{t}{b}\sin\phi - \frac{it_\beta}{b}\cos\phi. \tag{9.3}$$

If we now define r_α, r_β through

$$\left.\begin{aligned} x_1 - y_1 &= r_\beta\cos\phi + r_\alpha\cos\vartheta; \\ y_2 = r_\beta\sin\phi; &\quad x_2 = r_\alpha\sin\vartheta, \end{aligned}\right\} \tag{9.4}$$

we identically satisfy $\tau^{SP} = t$ when

$$\frac{r_\alpha}{a} + \frac{r_\beta}{b} = 1. \tag{9.5}$$

In essence, equations (9.2), (9.4) and (9.5) determine the six quantities ϑ, ϕ, a, b, r_α, r_β as functions of $\mathbf{x}$, $\mathbf{y}$ and t. They have the geometrical interpretation shown in Fig. 3. In Fig. 3, we may think of $\mathbf{y}_\alpha^*$ and $\mathbf{x}_\beta^*$ as image points for the *SP* phase. The

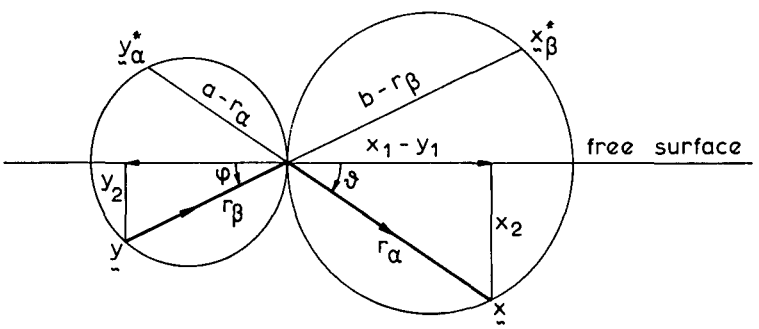

Fig. 3. The ray-paths and image systems for the reflected *SP*-phase, with angle of incidence ϕ and angle of reflection ϑ.

https://doi.org/10.1017/S1446181100001772 Published online by Cambridge University Press

path $\mathbf{y}_\alpha^*$ to $\mathbf{x}$ corresponds to an equivalent P wave; the path $\mathbf{y}$ to $\mathbf{x}_\beta^*$ to an equivalent S wave. The term $\dot{p}$ is found to be

$$\dot{p} = i\left[\frac{t_\alpha r_\alpha}{a\eta_\alpha} + \frac{t_\beta r_\beta}{b\eta_\beta}\right]^{-1}. \tag{9.6}$$

The SP first motion corresponds to

$$t = \frac{a}{\alpha} = \frac{b}{\beta} = \frac{r_\beta}{\beta} + \frac{r_\alpha}{\alpha}; \quad p = \frac{\cos\phi}{\beta} = \frac{\cos\vartheta}{\alpha}. \tag{9.7}$$

The last of these is the usual Snell's law of reflection.

Expanding about $t \gtrsim (r_\beta/\beta) + (r_\alpha/\alpha) = t_{SP}$ we find

$$G_{ik}(SP) \sim \frac{Q}{(2\alpha)^{\frac{1}{2}}\pi} \hat{r}_i(\vartheta)\hat{\theta}_k^*(\phi)\mathscr{R}_{SP}(\phi)\Gamma_{SP}(t-t_{SP})^{-\frac{1}{2}}, \tag{9.8}$$

where the SP-reflection coefficient

$$\mathscr{R}_{SP} = \frac{4\tan\phi(\tan^2\phi - 1)}{(\tan^2\phi - 1)^2 + 4\tan\vartheta\tan\phi}, \tag{9.9}$$

for incident angle ϕ and reflection angle ϑ. The geometrical spreading factor is given by

$$\Gamma_{SP} = \frac{r_\beta x_2[(\alpha/\beta)r_\beta + r_\alpha]^{\frac{1}{2}}}{y_2 r_\alpha^2 + x_2 r_\beta^2}. \tag{9.10}$$

The unit polarization vector $\hat{r}_i(\vartheta) = (\cos\vartheta, \sin\vartheta)$ relative to the image $\mathbf{y}_\alpha^*$. The source directivity $\hat{\theta}_k^*(\phi) = -(\sin\phi, \cos\phi)$ relative to the image $\mathbf{x}_\beta^*$.

The analysis for the PS phase is much the same, as would be expected by reciprocity. In place of equation (9.4) we set

$$\left.\begin{aligned} x_1 - y_1 &= r_\alpha\cos\vartheta + r_\beta\cos\phi; \\ y_2 &= r_\alpha\sin\vartheta; \quad x_2 = r_\beta\sin\phi. \end{aligned}\right\} \tag{9.11}$$

The first motion is found to be

$$G_{ik}(PS) \sim \frac{Q}{(2\beta)^{\frac{1}{2}}\pi} \hat{\theta}_i(\phi)\hat{r}_k^*(\vartheta)\mathscr{R}_{PS}(\vartheta)\Gamma_{PS}(t-t_{PS})^{-\frac{1}{2}}, \tag{9.12}$$

near

$$t \gtrsim \frac{r_\alpha}{\alpha} + \frac{r_\beta}{\beta} = t_{PS}.$$

The corresponding reflection coefficient (angle of incidence ϑ, angle of reflection ϕ) and geometrical spreading factor are given respectively by

$$\mathscr{R}_{PS}(\vartheta) = -\frac{4\tan\vartheta\,(\tan^2\phi - 1)}{(\tan^2\phi - 1)^2 + 4\tan\vartheta\tan\phi} \tag{9.13}$$

https://doi.org/10.1017/S1446181100001772 Published online by Cambridge University Press

and

$$\Gamma_{PS} = \frac{r_\alpha x_2[(\beta/\alpha)r_\alpha + r_\beta]^{\frac{1}{2}}}{x_2 r_\alpha^2 + y_2 r_\beta^2}. \tag{9.14}$$

10. The Rayleigh wave on the free surface

We observe that the expressions for PP, SP, PS and SS in the Pekeris–Cagniard–de Hoop representation (5.9) each contains the common factor $R^{-1}(p)$. The equation $R(p) = 0$ is the classical Rayleigh equation with root $p = 1/\gamma$ where $\gamma\ (<\beta<\alpha)$ is the Rayleigh wave speed. Dominant contributions to the Green's tensor will arise when $R(p)$ is near zero. This condition eventuates for $x_2 = 0$; $y_2 \ll |x_1 - y_1| = r$, say. On $x_2 = 0$, $\tau^{PP} = \tau^{PS}$ and $\tau^{SP} = \tau^{SS}$. Expanding about the surface slowness $p \sim 1/\gamma$ we find, after much simplification,

$$G_{ik}(R) \sim \frac{-Q}{2\pi R'(1/\gamma)}\left[\frac{\alpha_{ik}(t-r/\gamma)+a_{ik}\zeta_\alpha y_2}{(t-r/\gamma)^2+\zeta_\alpha^2 y_2^2} + \frac{\beta_{ik}(t-r/\gamma)+b_{ik}\zeta_\beta y_2}{(t-r/\gamma)^2+\zeta_\beta^2 y_2^2}\right]. \tag{10.1}$$

where

$$\left.\begin{aligned} \alpha_{ik} &= \begin{pmatrix} \dfrac{A}{\gamma\zeta_\alpha} & 0 \\ 0 & -\gamma\zeta_\alpha B \end{pmatrix}; \quad a_{ik} = \begin{pmatrix} 0 & A \\ B & 0 \end{pmatrix}; \\ \beta_{ik} &= \begin{pmatrix} -\gamma\zeta_\beta B & 0 \\ 0 & \dfrac{A}{\gamma\zeta_\beta} \end{pmatrix}; \quad b_{ik} = \begin{pmatrix} 0 & -B \\ -A & 0 \end{pmatrix}; \end{aligned}\right\} \tag{10.2}$$

and

$$\left.\begin{aligned} A &= \frac{4\zeta_\alpha\zeta_\beta}{\gamma\beta^2}; \qquad B = \frac{4(\zeta_\alpha\zeta_\beta)^{\frac{1}{2}}}{\gamma^2\beta^2}; \\ \zeta_\alpha &= \left(\frac{1}{\gamma^2}-\frac{1}{\alpha^2}\right)^{\frac{1}{2}}; \quad \zeta_\beta = \left(\frac{1}{\gamma^2}-\frac{1}{\beta^2}\right)^{\frac{1}{2}}. \end{aligned}\right\} \tag{10.3}$$

There is no sharp onset for the Rayleigh wave and the surface particle motion will be a very complicated elliptic type of motion.

11. Other diffracted arrivals

Lapwood [13] theoretically discovered a set of asymptotic diffracted phases neither mentioned nor found in many of the subsequent analyses of the Lamb's problem. Our exact solution predicts the existence of these phases. They can occur

only in the case $x_2+y_2 \ll |x_1-y_1| = r$ when Γ lies close to the positive real p-axis, and correspond to surface slownesses coincident with the P and S wave slownesses $1/\alpha$ and $1/\beta$. Their amplitudes are found to vary like $r^{-\frac{1}{2}}(t-r/\alpha, \beta)^{\frac{1}{2}}$ near $t = r/\alpha, \beta$ and are therefore of minor significance compared to the other principal arrivals considered.

In Table 1 we show the correspondence between Lapwood's phases and the potentials and surface slownesses from which they derive.

TABLE 1

Lapwood's 1949 phases	Associated potential	Surface slowness p
pSp	$\phi_1(PP)$	$1/\beta$
sP	$\Omega(SP)$	$1/\alpha$
pS	$\chi(PS)$	$1/\beta$
Sp	$\Omega(SP)$	$1/\beta$
Ps	$\chi(PS)$	$1/\alpha$

The last two, which were not considered by Lapwood, should also exist according to our solution. These are the reciprocal phases to sP and pS respectively.

12. Dipolar sources

The elastic displacements generated by dipolar (or multipolar) line sources may be obtained by appropriate differentiation with respect to source coordinates $\mathbf{y}$.

Thus the displacement field given by $u_i^{kl} = \partial_0^l G_{ik}$ is that for a dipole with k defining the force direction and l the dipole axis.

The Pekeris–Cagniard–de Hoop representation then gives the following expressions for the radiated waves:

$$\left.\begin{aligned} u_i^{kl}(P) &= \frac{Q}{2\pi}\frac{\partial}{\partial t}\,\mathrm{Im}\,[\pi_i^{\pm}\,\pi_k^{\pm}\,\pi_l^{\pm}\,\dot{p}/\eta_\alpha]_{\tau^P=t}; \\ u_i^{kl}(S) &= \frac{Q}{2\pi}\frac{\partial}{\partial t}\,\mathrm{Im}\,[\sigma_i^{\pm}\,\sigma_k^{\pm}\,s_l^{\pm}\,\dot{p}/\eta_\beta]_{\tau^S=t}. \end{aligned}\right\} \tag{12.1}$$

The first motions corresponding to these are

$$\left.\begin{aligned} u_i^{kl}(P) &\sim \frac{-Q}{(2\alpha)^{\frac{1}{2}}\pi}\hat{r}_i(\hat{r}_k\hat{r}_l)\,r^{-\frac{1}{2}}(t-r/\alpha)^{-\frac{1}{2}}, \quad t \gtrsim r/\alpha; \\ u_i^{kl}(S) &\sim \frac{-Q}{(2\beta)^{\frac{1}{2}}\pi}\hat{\theta}_i(\hat{\theta}_k\hat{r}_l)\,r^{-\frac{1}{2}}(t-r/\beta)^{-\frac{1}{2}}, \quad t \gtrsim r/\beta. \end{aligned}\right\} \tag{12.2}$$

https://doi.org/10.1017/S1446181100001772 Published online by Cambridge University Press

Comparison with the simple line source (equation (6.5)) is instructive. First, the wave-front singularities for the dipole source are more severe and the radiation patterns $\hat{r}_k \hat{r}_l$ and $\hat{\theta}_k \hat{r}_l$ will be more structured. The S to P amplitude ratio is $(\alpha/\beta)^{\frac{1}{2}}$ so that dipolar sources enhance S wave generation. Polarization vectors and geometrical spreading will be the same for all multipole sources. Other possibilities also come to mind. The displacement field $u_i^{kl} = \partial_0^l G_{ik} + \partial_0 G_{il}$ corresponds to the double-couple line source (Burridge and Knopoff [2]). The summed dipoles (over the index k) $u_i^P = \partial_0^k G_{ik}$ and $u_i^S = \partial_0^k \mathrm{G}_{ik}$ generate pure P and S waves respectively. They have the first motions given by (12.2) with unit radiation pattern; that is uniform source directivity.

References

[1] A. Ben-Menahem and M. Vered, "Extension and interpretation of the Cagniard–Pekeris method for dislocation sources", *Bull. Seism. Soc. Amer.* 63 (1973), 1611–1636.

[2] R. Burridge and L. Knopoff, "Body force equivalents for seismic dislocations", *Bull. Seism. Soc. Amer.* 54 (1964), 1875–1888.

[3] R. Burridge, E. R. Lapwood and L. Knopoff, "First motions from seismic sources near a free surface", *Bull. Seism. Soc. Amer.* 54 (1964), 1889–1913.

[4] L. Cagniard, *Reflexion et refraction des ondes seismiques progressives* (1939). English translation by E. A. Flinn and C. J. Dix (McGraw-Hill, International Series in the Earth Sciences, 1962).

[5] A. T. de Hoop, "A modification of Cagniard's method for solving seismic pulse problems", *Appl. Sci. Res., B* 8 (1962), 349–356.

[6] G. Eason, J. Fulton and I. N. Sneddon, "The generation of waves in an infinite elastic solid by variable body forces", *Phil. Trans., A* 248 (1956), 576–607.

[7] H. G. Garnir, "Propagation de l'onde émise par une source ponctuelle et instantanée dans un dioptre plan", *Bull. Soc. Roy. Sci. Liège* 3/4 (1953), 85–100/148–162.

[8] W. W. Garvin, "Exact transient solution of the buried line source problem", *Proc. Roy. Soc. Lond., A* 234 (1956), 528–541.

[9] F. Gilbert and L. Knopoff, "The directivity problem for a buried line source", *Geophys.* 26 (1961), 626–634.

[10] L. R. Johnson, "Green's function for Lamb's problem", *Geophys. J. R. Astr. Soc.* 37 (1974), 99–131.

[11] D. W. King, R. A. W. Haddon and E. S. Husebye, "Precursors to *PP*", *Phys. Earth Planet. Ints.* 10 (1975), 103–127.

[12] H. Lamb, "On the propagation of tremors over the surface of an elastic solid", *Phil. Trans. A* 203 (1904), 1–42.

[13] E. R. Lapwood, "The disturbance due to a line source in a semi-infinite medium", *Phil. Trans A* 242 (1949), 63–100.

[14] H. Nankano, "On Rayleigh waves", *Jap. J. Astr. Geophys.* 2 (1925), 233–326.

[15] C. L. Pekeris, "The seismic surface pulse", *Proc. Nat. Acad. Sci.* 41 (1955), 469–480.

[16] C. L. Pekeris, "The seismic buried pulse", *Proc. Nat. Acad. Sci.* 41 (1955), 629–639.

Department of Applied Mathematics
University of Sydney
N.S.W., Australia, 2006